Acta Crystallographica Section D
Biological Crystallography
ISSN 0907-4449

Crystallization and preliminary X-ray diffraction studies on the DNA-binding domain of the multidrug transporter activation protein (MtaN) from *Bacillus subtilis*

Michael H. Godsey,[a] Natalya N. Baranova,[b] Alexander A. Neyfakh[b] and Richard G. Brennan[a]*

[a]Department of Biochemistry and Molecular Biology, Oregon Health Sciences University, 3181 SW Sam Jackson Park Road, Portland, Oregon, 97201-3098, USA, and [b]Center for Pharmaceutical Biotechnology, University of Illinois, Chicago, Illinois, 60607, USA

Correspondence e-mail: brennanr@ohsu.edu

Received 2 May 2000
Accepted 24 July 2000

The N-terminal DNA-binding domain of the multidrug transporter activation protein (MtaN) was crystallized by the hanging-drop vapour-diffusion method using lithium chloride as a precipitant. The crystals are orthorhombic and belong to the space group $I2_12_12_1$, with unit-cell parameters a = 49.4, b = 67.8, c = 115.0 Å. Diffraction data have been collected at 100 K to 2.75 Å resolution at a synchrotron-radiation source.

1. Introduction

Bacteria express a variety of membrane-bound proteins that extrude toxins from the cell. Because the recognized compounds include many antibiotics, these proteins have been named multidrug transporters (Paulsen *et al.*, 1996; van Veen *et al.*, 1999). In *Bacillus subtilis*, two of these proteins, Bmr and Blt, have been shown to be controlled by specific transcriptional regulators, BmrR and BltR, respectively (Ahmed *et al.*, 1994, 1995). However, both transporters are further regulated by the multidrug transporter activation protein (Mta; Baranova *et al.*, 1999). This protein also controls its own transcription and that of at least one more gene, *ydfK*, which encodes a putative membrane protein.

Mta, like BmrR and BltR, is a member of the MerR family, named for the mercury-resistance gene regulator (Summers, 1992; Hidalgo *et al.*, 1997). This family has high sequence conservation in the N-terminal DNA-binding domain, which is predicted to contain a helix–turn–helix DNA-binding motif. However, the C-terminal domains of the family are widely divergent in both size and sequence. Beyond the helix–turn–helix motif, there appears to be no sequence or structural homology between the members of the MerR family and any other gene regulators.

Mta contains 257 residues and is a functional dimer. A truncated form of Mta, encompassing the first 109 amino acids (MtaN), is able to bind to the promoter elements and activate the transcription of genes under control of the full-length protein (Baranova *et al.*, 1999). Thus, it appears that the C-terminus contains a regulatory domain, removal of which is sufficient to relieve inhibition of transcriptional activation. *In vivo*, MtaN activates its own transcription, creating a positive feedback loop leading to high levels of intracellular protein. This may be important, as our binding studies have found that MtaN has 30- to 50-fold higher K_d values for the *bmr* and *blt* promoters, respectively, than for the *mta* promoter (data not shown).

Our interest in MtaN is twofold. The promoters targeted by MerR family members contain an unusually long 19 base-pair spacer between the −10 and −35 elements, and the structural mechanism of transcriptional activation by this family remains unclear. In addition, the known promoter targets of MtaN are quite dissimilar, with only 12 consensus base pairs in a stretch of 31, of which only six are found in the DNase I footprint of the protein (Baranova *et al.*, 1999). Such limited base-pair conservation suggests an unusual mechanism of multiple promoter recognition.

To understand the molecular mechanism of transcription activation by MerR family members and multiple promoter recognition by a single protein, we have undertaken experiments to determine the three-dimensional structure of MtaN by X-ray diffraction methods. In this paper, we report the crystallization and preliminary X-ray diffraction analysis of the DNA-binding domain of the MerR family member Mta.

2. Experimental results and discussion

2.1. Purification and solubilization

Expression and purification of MtaN in *Escherichia coli* was performed essentially as described in Baranova *et al.* (1999). 1 l of cells expressing MtaN fused to a C-terminal six-histidine tag was pelleted, resuspended in ∼25 ml of lysis buffer (20 m*M* bis-tris propane pH 8.9, 250 m*M* NaCl) and lysed in a French pressure cell at 68.9 MPa. Lysates clarified by centrifugation were added to 4 ml of a 50% slurry of Talon cobalt-affinity resin (Clonetech) and purified by a hybrid batch-gravity flow method. Briefly, the clarified lysates were mixed with a resin slurry, allowed to bind and

Table 1
Data statistics.

Values in parentheses refer to the outer shell.

Crystal	Native	Se-Met			
SSRL† beamline	7-1	1-5			
Unit-cell parameters (Å)	a = 49.4, b = 67.8, c = 115.0	a = 50.1, b = 67.6, c = 116.1			
Resolution limits (Å)	23.30–2.75	58.72–2.90			
Outer shell (Å)	2.82–2.75	2.98–2.90			
Wavelength (Å)	1.08	0.9226	0.97945	0.97988	1.06883
Observed reflections	42297	18361	18945	19064	18568
Unique reflections	5199	4502	4515	4523	4497
Completeness (%)	99.3 (99.0)	97.0 (100)	97.3 (100)	97.4 (100)	96.9 (93.5)
Mean $I/\sigma I$	7.9 (2.7)	4.2 (1.4)	4.0 (1.5)	6.4 (1.6)	5.1 (2.0)
R_{sym}‡ (%)	7.2 (27.1)	6.7 (51.0)	6.8 (51.2)	5.3 (48.6)	5.1 (38.1)

† Standford Synchrotron Radiation Laboratory. ‡ $R_{sym} = \sum|I_o - I_{avg}|/\sum I_o$.

washed several times. The resin was then poured into a small gravity-flow column for stepwise elution. Protein was eluted with 50 m*M* imidazole and fractions containing MtaN were combined and dialyzed against storage buffer (20 m*M* bis-tris propane pH 8.9, 100 m*M* NaCl). The solubility of the protein was found to be inadequate for crystallization below pH 8.5. Subsequent dynamic light-scattering experiments indicated enhanced solubility and monodispersity at pH values $\geq$8.9. The protein was concentrated to $\sim$11 mg ml^{-1} in a Centricon 3 and used for crystallization experiments. 1 l of culture yields approximately 20 mg of pure protein.

2.2. Crystallization

Crystallization conditions were screened by vapour diffusion using the hanging-drop method. Droplets which contained 2 µl each of protein and reservoir solution were equilibrated over 1 ml of reservoir solution at room temperature. Crystals were obtained in 2 d from a reservoir solution of 3.77 *M* LiCl, 50 m*M* HEPES pH 7.0, 10 m*M* $MgCl_2$. A 20 µl drop yields one or two crystals with dimensions of approximately 0.4 × 0.4 × 0.6 mm in a few days (Fig. 1). These crystals were found to be too unstable for data collection at room temperature. In one attempt to lengthen the lifetime of these crystals, drops containing single crystals were removed from their wells, placed over reservoirs containing 5.0 *M* LiCl in the crystallization buffer and allowed to re-equilibrate. Surprisingly, these crystals typically doubled in size overnight and their lifetime in the beam was increased enough to allow the determination of unit-cell parameters and limit space-group choice to one of two. However, for complete data collection the crystals must be frozen. A systematic search for a good cryo-protectant revealed that the crystallization solution alone, containing 3.77 *M* LiCl, is quite effective for protection.

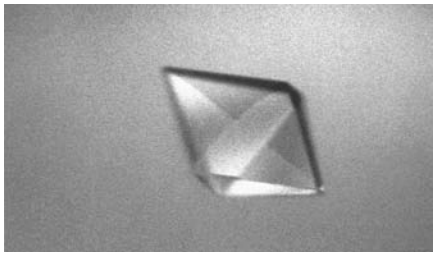

Figure 1
A crystal of MtaN. This crystal is approximately 0.8 mm long.

2.3. X-ray diffraction

Preliminary intensity data for unit-cell parameter and space-group determination were collected on an R-AXIS IV image-plate system equipped with double-focusing mirrors and using Cu $K\alpha$ radiation from a Rigaku RU-300 rotating-anode generator operated at 50 kV and 100 mA. These data revealed an orthorhombic space group, either $I222$ or $I2_12_12_1$, which are indistinguishable from each other based on diffraction patterns. A V_M value of 3.6 Å^3 Da^{-1} (Matthews, 1968) and a solvent content of 63% are consistent with a single molecule in the asymmetric unit. There is a band of diffuse scattering in the diffraction pattern at resolutions between 4.0 and 3.0 Å (Fig. 2). The cause of this is unclear, although it is likely to be a consequence of thermal motion in the crystal lattice. All experimental attempts to eliminate this feature have failed. However, the thermal diffusion does not seem to interfere significantly with successful data collection and intensity integration.

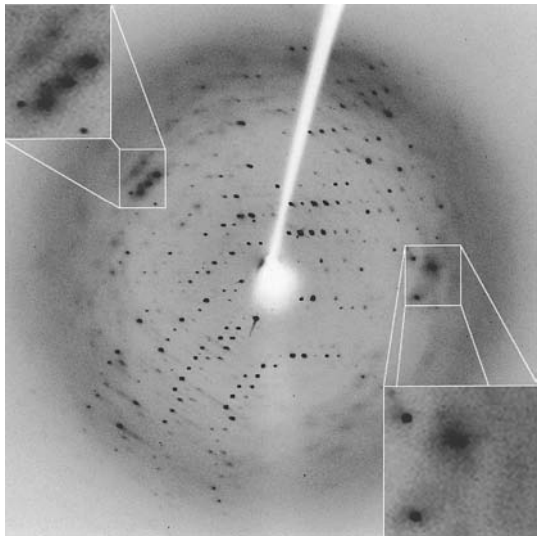

Figure 2
A diffraction image of MtaN. Insets show a threefold magnification of diffuse scattering in the 4.0–3.7 Å resolution shell.

Although the crystals are very unstable in the X-ray beam at room temperature, they are extremely stable in the crystallization drop. As an example, the best intensity data have been collected from a crystal over 18 months old (Table 1). For intensity data collection, a crystal was removed directly from the drop in which it was grown, flash-frozen in the N_2 stream of an X-stream cryo-cooling system (Molecular Structure Corporation) and stored until data collection. Intensity data were collected at 100 K on beamline 7-1 at the Stanford Synchrotron Radiation Laboratory (SSRL) using a MAR 345 detector and λ = 1.08 Å. Intensity data were processed and scaled using *MOSFLM* (Collaborative Computational Project, Number 4, 1994).

Heavy-atom soaks have been unsuccessful in derivatizing the protein, although this may in part be a consequence of the presence of the high salt concentration in the crystallization conditions. As an alternative strategy, selenomethionyl-substituted protein has been prepared (Van Duyne *et al.*, 1993) for use in multiwavelength anomalous diffraction (MAD) experiments (Hendrickson, 1991) and has yielded data-quality crystals. A MAD intensity data set has been collected using beamline 1-5 at SSRL (Table 1).

Patterson map analysis of the MAD data using *SOLVE* (Terwilliger & Berendzen, 1999) has located four of the five possible selenium sites and shown the space group to be $I2_12_12_1$, rather than the far more commonly observed space group $I222$. Initial electron-density

maps show clear protein and solvent regions. Solvent flattening in *PHASES* (Furey & Swaminathan, 1997) has significantly improved the quality of these maps and model building is under way.

References

Ahmed, M., Borsch, C. M., Taylor, S. S., Vazquez-Laslop, N. & Neyfakh, A. A. (1994). *J. Biol. Chem.* **269**, 28506–28513.

Ahmed, M., Lyass, L., Markham, P. N., Taylor, S. S., Vazquez-Laslop, N. & Neyfakh, A. A. (1995). *J. Bacteriol.* **177**, 3904–3910.

Baranova, N. N., Danchin, A. & Neyfakh, A. A. (1999). *Mol. Microbiol.* **31**, 1549–1559.

Collaborative Computational Project, Number 4 (1994). *Acta Cryst.* D**50**, 760–763.

Furey, W. & Swaminathan, S. (1997). *Methods Enzymol.* **277**, 590–620.

Hendrickson, W. A. (1991). *Science*, **254**, 51–58.

Hidalgo, E., Ding, H. & Demple, B. (1997). *Trends Biochem Sci.* **22**, 207–210.

Matthews, B. W. (1968). *J. Mol. Biol.* **33**, 491–497.

Paulsen, I. T., Brown, M. H. & Skurray, R. A. (1996). *Microbiol. Rev.* **60**, 575–608.

Summers, A. O. (1992). *J. Bacteriol.* **174**, 3097–3101.

Terwilliger, T. C. & Berendzen, J. (1999). *Acta Cryst.* D**55**, 849–861.

Van Duyne, G. D., Standaert, R. F., Karplus, P. A., Schreiber, S. L. & Clardy, J. (1993). *J. Mol. Biol.* **229**, 105–124.

Veen, H. W. van, Putman, M., Margolles, A., Sakamoto, K. & Konings, W. N. (1999). *Biochem. Biophys. Acta*, **1461**, 201–206.